J Mater Sci (2011) 46:3802–3811
DOI 10.1007/s10853-011-5294-1

Young's modulus and damping in dependence on temperature of Ti–6Al–4V components fabricated by shaped metal deposition

Akhilesh Kumar Swarnakar · Omer van der Biest · Bernd Baufeld

Received: 9 November 2010 / Accepted: 14 January 2011 / Published online: 29 January 2011

Abstract Young's modulus and damping behavior is investigated by the impulse excitation technique in vacuum up to 1100 °C for Ti–6Al–4V components, fabricated by shaped metal deposition (SMD). This is a novel additive manufacturing technique where near net-shape components are built layer by layer by tungsten inert gas welding. The Young's modulus decreases linearly from 118 GPa at room temperature to 72 GPa at 900 °C, followed by a stronger decrease up to 1000 °C and during the first heating a plateau thereafter. The damping exhibits an exponential increase with temperature superimposed by two peaks around 700 and 900 °C during the first heating. During cooling and follow-up cycles only the damping peak around 700 °C appears. The change in Young's modulus and the damping behavior is interpreted by different processes like α/β transformation, O alloying and grain boundary sliding. These results indicate that components fabricated by SMD contain a non-equilibrium α phase which transforms to the β phase at higher temperatures than the equilibrium α phase. Furthermore, the vacuum between 2.4 and 5.3 $\times$ 10^{-4} mbar proved at high temperatures to be not good enough to rule out the contamination by O, which leads to α casing, stiffening, and hardening.

A. K. Swarnakar · O. van der Biest
MTM, Katholieke Universiteit Leuven, Kasteelpark Arenberg 44, 3001 Leuven, Belgium
e-mail: AkhileshKumar.Swarnakar@mtm.kuleuven.be

O. van der Biest
e-mail: Omer.VanderBiest@mtm.kuleuven.be

B. Baufeld (✉)
NAMRC, University of Sheffield, Brunel Way, Rotherham S60 5WG, United Kingdom
e-mail: b.baufeld@namrc.co.uk

Abbreviations

SMD	Shaped metal deposition
IET	Impulse excitation technique
TIG	Tungsten inert gas
SEM	Scanning electron microscopy
BSE	Backscattered electron
EDX	Energy dispersive X-ray
IGA	Instrumental gas analysis

Introduction

Titanium alloys are widely used in aerospace industry due to their excellent strength/weight ratio [1] and in medical industry due the superior biocompatibility, low elastic modulus, and enhanced corrosion resistance [2]. Especially in case of aerospace applications, e.g., gas turbine engines, the mechanical behavior at elevated temperatures is of interest.

Generally, Ti is an expensive metal and traditional machining of Ti alloys is money and time consuming. Innovative manufacture routes which would reduce the amount of scrap and the time to flight would be of great advantage. Shaped metal deposition (SMD) is a near net-shape welding technique [3], patented by Rolls-Royce, where fully dense metal parts are fabricated by welding successively layer by layer. This additive layer manufacturing allows rapid fabrication of three dimensional objects directly from a computer aided design data source. This approach will have a major impact on the design of parts. Furthermore, this technique promises to be applied in the small scale production of parts and for repair of high performance alloy components. While traditional methods such as forging or machining subtract a large amount of

metal from a work piece to obtain a desired shape, SMD omits this destructive, time consuming, and costly process by adding material progressively to create a near-net shaped component. SMD parts need minimal finishing and low scrap rates can be achieved, which is particularly advantageous in the case of Ti alloys due to their high material costs and difficult machinability.

Before application of a component fabricated by a novel fabrication route the designer has to know the material properties. Since Ti is sensitive to the thermal history, and SMD exhibits a rather peculiar fabrication scheme with repeated exposure to high temperatures and thermal gradients, simple deduction of the properties from Ti alloys fabricated by conventional techniques is not possible. Preliminary results for Ti–6Al–4V SMD components, one of the most widely used $\alpha + \beta$ Ti alloys, are already published elsewhere with the emphasis on microstructure and mechanical properties [4, 5]. The subject of this article is to study directly the dependence of Young's modulus and damping on temperature by means of the impulse excitation technique (IET) [6, 7]. Such measurements do not only provide these material properties, but may also give some insight into energy consuming processes such as phase transformation.

Experimental procedure

SMD

The SMD cell, located at the AMRC, Sheffield, United Kingdom, consists of a tungsten inert gas (TIG) welding head, attached to a 6-axis Kuka robot linked to a 2-axis table, all of which are enclosed in an airtight chamber. Cold wire TIG deposition is used to weld Ti–6Al–4V wire with a diameter of 1.2 mm in an inert argon atmosphere. Argon is controlled to 99.999% purity and moisture is also controlled to maintain part integrity. As demonstrated in Table 1, the SMD component has a similar N and O contamination as the wire. The controlled SMD parameters include the wire feed speed of 2.4 m/min, the table speed of 0.3 m/min and the electrical current of 150 A. The component is created by laying down a weld layer by layer with a step height of 1 mm and rotating the table to keep a constant torch direction. For this case the result is a tubular shape with squared cross section (0.15×0.15 m^2), a height of 0.12 m, and a wall width of 0.01 m.

Table 1 N and O concentration of the Ti–6Al–4V wire, the SMD component and inside specimen E1 after IET testing

Specimens	N (wt%)	O (wt%)
Wire	0.0030	0.142
SMD component	0.0041	0.160
Specimen E1 after IET	0.0021	0.370

For IET, small bars with coplanar sides have been prepared. Specimens parallel and perpendicular to the deposition plane have been tested (Table 2). In addition, one specimen (F) was heat treated within an evacuated and sealed glass ampoule at 1100 °C for 4 h and water quenched to obtain martensite.

IET

The dynamic Young's modulus and the damping were measured by the IET [6–8]. IET measures the fundamental resonant frequency of a specimen of suitable geometry by exciting it mechanically with an impulse tool. The resonance frequencies are characteristic for the test object, as they are related to its stiffness, mass and geometry. Figure 1 shows a sketch of the IET fixture with the suspended rectangular specimen, appropriate for flexural mode measurements [8]. The set-up of the suspension is designed to counteract the different thermal expansions of the different components during the high temperature experiment and to keep the specimen in place. The suspension is accomplished by weights and carbon wires fixing the specimen at its vibration nodes. The mechanical excitation is achieved by a ceramic rod hitting automatically the specimen from below at the center at a predescribed (usually 2 min) rate.

A transducer (in the case of vacuum a laser based vibrometer) senses the resulting mechanical vibrations of the specimen and transforms them into electric signals.

According to the ASTM standard [8] in the case of isotropic samples of rectangular shape with appropriate dimensions, the Young's modulus E can be calculated as:

$$E = 0.9465 \times \left[\frac{m \times f_r^2}{b}\right] \times \left(\frac{L}{t}\right)^3, \quad (1)$$

where f_r represents the resonance frequency and m the mass of the sample. L, b, and t are the dimensional units (length, width, and thickness).

The vibration can also be analyzed from the internal friction (Q^{-1}) point of view, i.e., the dissipation of vibration energy in the specimen, or damping, or mechanical loss. Q^{-1} can be deduced from the amplitude decay of a free vibration. Damping is closely related to the integral mechanisms of dissipation of the mechanical energy in the material. The exact microstructural origin of damping or mechanical loss changes from one material to another.

The high temperature IET tests were performed in a graphite furnace HTVP-1750C in vacuum (better than 10^{-3} mbar) and analyzed by the RFDA software (both IMCE, Diepenbeek, Belgium). The Young's modulus and

Table 2 Denomination and details of IET specimens, vacuum during the experiment, Young's modulus E at different temperatures, and the damping peak temperatures (na: not applicable or not analyzed)

Specimen	Orientation	Dimension (mm^3)	Vacuum 10^{-4} mbar	Young's modulus E (GPa)				At temperature (°C)	
				Before IET	During heating		After cooling		
				At room temperature	At 900 °C	At 1000 °C	At room temperature	Peak 1	Peak 2
A1	Perpendicular	37.7 × 8.0 × 2.9	na	117	66	57	125	na	na
B1	Perpendicular	37.6 × 8.0 × 3.0	na	117	69	59	124	719	877
B2	Perpendicular	35.1 × 7.7 × 2.8	3.2	126	81	71	na	na	na
C1	Perpendicular	37.8 × 7.8 × 2.9	na	118	69	55	123	713	890
D1	Parallel	53.3 × 6.9 × 2.9	6.5	118	71	64	127	666	858
E1	Parallel	39.6 × 7.8 × 2.9	2.4	119	77	72	120	698	864
F0	Parallel	38.4 × 7.5 × 2.8	na	116	na	na	na	na	na
F1 martensite	Parallel	34.2 × 7.3 × 2.6	4.8	102	64	57	110	749	827

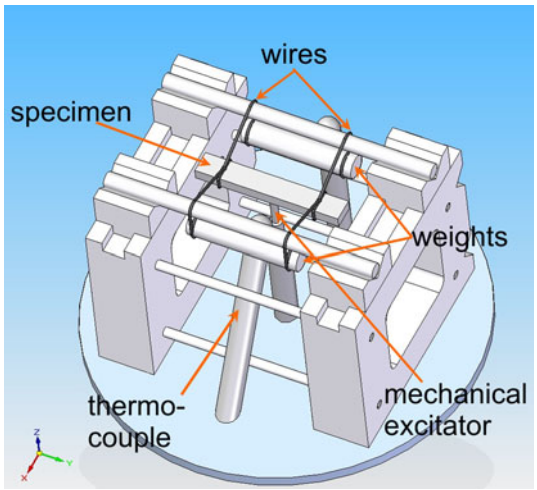

Fig. 1 Sketch of IET fixture including suspended specimen (courtesy to Marc Nolmans, MTM, Katholieke Universiteit Leuven, Belgium)

the damping has been measured from room temperature up to 1100 °C with a heating and cooling rate of 2 K/min. Specimens with length axis perpendicular (A1, B1, C1) and parallel to the deposition plane (D1, E1, F1) were measured. The specimens were cut by electrical discharge machining, and ground and polished manually to avoid machining induced residual stresses. The dimensions of the specimens are given in Table 2. Specimen B was tested a second time (B2), after grinding off more than 0.1 mm of the surface on each side to remove possible surface contamination due to the first IET sequence. For one specimen the Young's modulus first has been measured at room temperature (F0) and then heat treated, as already described, at 1100 °C to obtain the martensite α' phase (F1). Before IET testing more than 0.1 mm surface material has been grinded off. This measure was taken, since during the fast cooling the glass tube broke and surface contamination could not be excluded.

The specimens were measured in flexural mode, which means that the Young's modulus is measured in the length direction. It must be emphasized that IET is more sensitive to the properties at the surface than at the center of the tested bar.

Other testing techniques

The microstructure was investigated by scanning electron microscopy (SEM, FEI XL30FEG) of polished cross sections, where back-scattered electron (BSE) imaging with very high contrast allows discerning directly the α and β phases omitting artifacts from etching. Energy dispersive X-ray (EDX) point analysis was applied to determine the composition. Since EDX is not suitable to measure lighter elements such as O, in addition the EPMA-WDS microprobe working at 15 kV was applied.

Furthermore, instrumental gas analysis (IGA) has been utilized by Shiva Technologies Europe SAS, France for highly accurate measurements of the O and N concentration.

The Vickers microhardness tests were performed on polished cross sections of as-fabricated, heat treated specimens, and specimens tested by IET applying a Leitz/Durimet 2 microhardness tester using a weight of 100 g (HV0.1).

Results

IET

At room temperature the Young's modulus of the as-fabricated specimens are very similar, independent on the orientation relative to the deposition direction, all in the

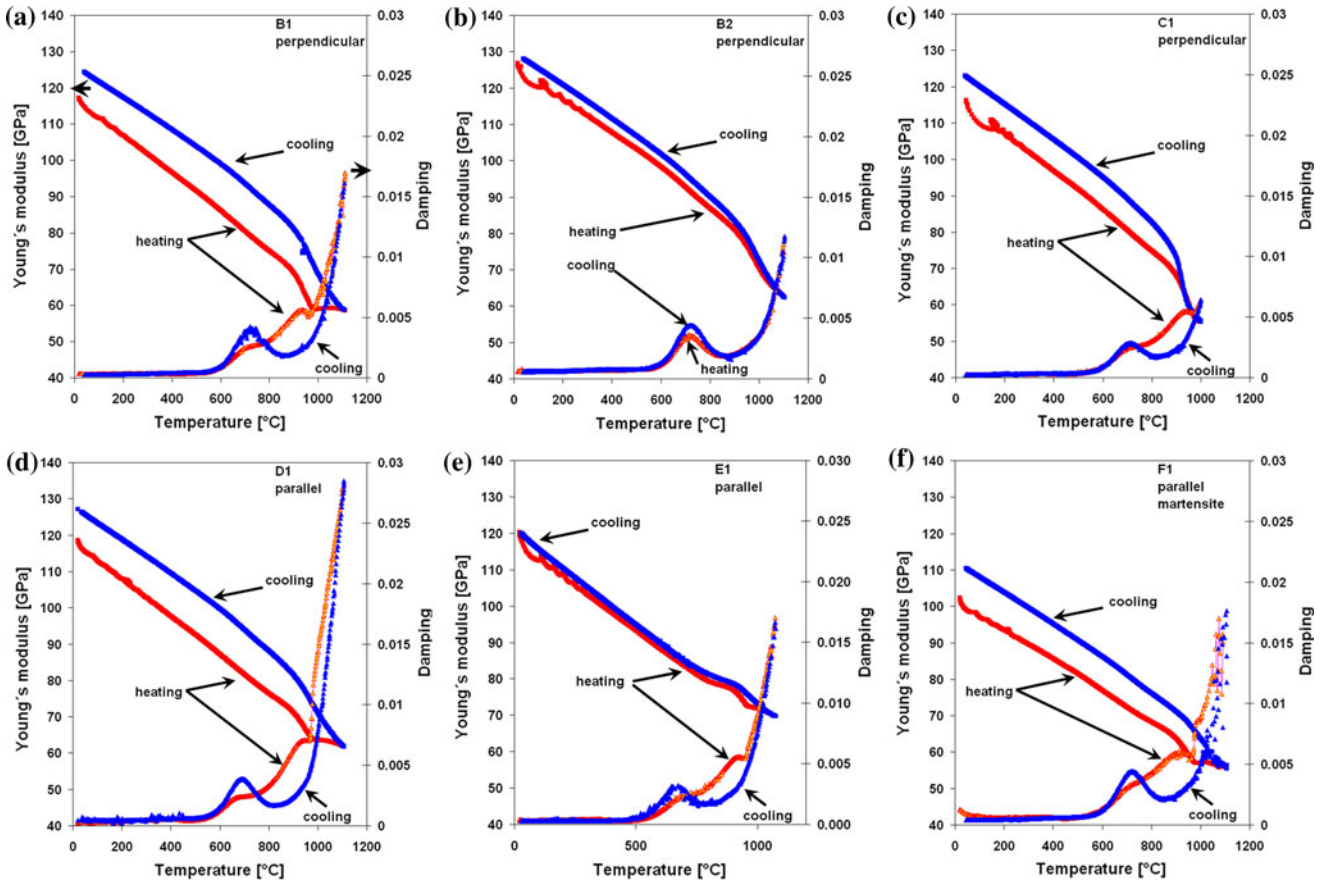

Fig. 2 Young's modulus (*squares*) and damping (*triangles*) (*arrows* indicate the respective ordinates) in dependence on temperature during heating and cooling. **a** and **b** First and second experiment of specimen B. **c** Specimen C tested only until 1000 °C. **d** Specimen D. **e** Specimen E. **f** Specimen F, originally martensite

order of about 118 GPa (Table 2). The magnitude agrees with published values for Ti–6Al–4V, where, depending on the O concentration, on the volume fraction of the different phases, and on the texture, values between 100 and 130 GPa are reported [9].

The heat treatment within the β phase field at 1100 °C, followed by water quenching, resulted in a decrease of the Young's modulus to 102 GPa (F1). Apparently, martensite of Ti–6Al–4V exhibits a lower stiffness (F1) than the $\alpha + \beta$ material before this treatment (F0).

For all tested SMD specimens, with increasing temperature the Young's modulus first decreases linearly until about 900 °C,[1] followed by a steep drop (Fig. 2). The average Young's modulus value of as-fabricated SMD specimens during the first heating sequence at 900 °C is 72 GPa. During the first heating, at around 950 °C this drop is stopped, and with further increasing temperature a plateau develops. This plateau is in some cases slightly tilted downwards (for example Fig. 2d). During subsequent cooling, the curves do not replicate this plateau but show first a steep and then a shallower slope, exhibiting a hysteresis behavior. The amount of hysteresis depends on the quality of the vacuum (Fig. 3) and the difference of the Young's module between heating and cooling increases linearly with increasing gas pressure. The influence of the quality of the vacuum is obvious comparing the curves of specimen D1 and E1, where the only difference is the vacuum pressure of 6.5 (specimen D1) and 2.4×10^{-4} mbar (specimen E1), respectively. It is therefore evident that the quality of the vacuum influences the hysteresis, and that for a good vacuum almost no hysteresis was obtained.

There is no difference between specimens with main axis parallel or perpendicular to the deposition layer (compare, for example Fig. 1a and d). The martensite specimen F1 (Fig. 2f) exhibits a similar behavior (but at lower values) than the as-fabricated $\alpha + \beta$ material.

An IET sequence only up to 1000 °C (C1) naturally does not show a plateau, but still a hysteresis during cooling (Fig. 2c).

[1] The loops visible at low temperature during heating are related with temperature control problems, where the real temperatures of the specimen differ with the measured values.

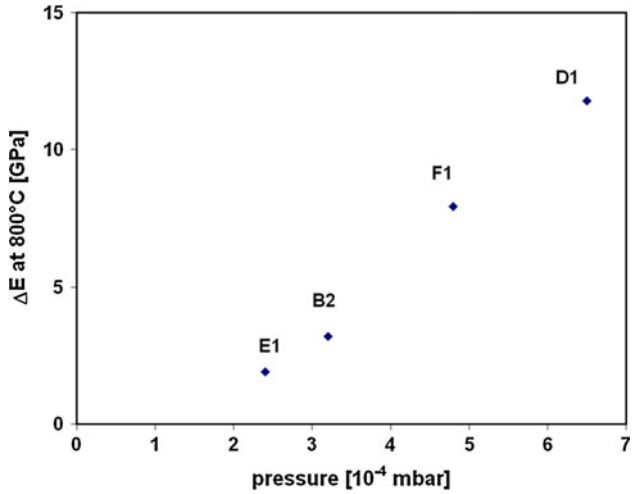

Fig. 3 Difference in Young's modulus between heating and cooling sequence (at 800 °C) in dependence of vacuum pressure

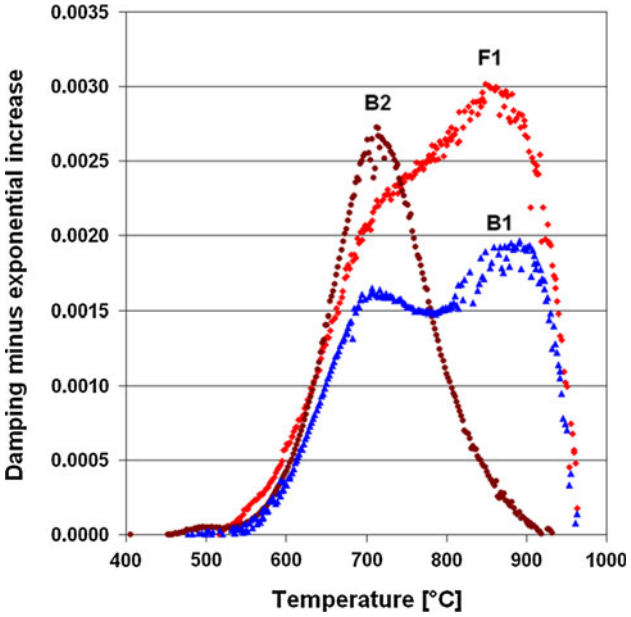

Fig. 4 Deconvolution of the damping by subtracting the exponential increase of the damping for specimens B1, B2, and F1

Testing a second time (B2), after removing more than 0.1 mm from all sides, the Young's modulus is shifted to higher values and the drop starts at higher temperatures (~950 °C) (Fig. 2b). This curve also exhibits no plateau, despite testing until 1100 °C. Furthermore, the hysteresis is relatively small.

The damping curves show for all specimens an exponential increase with temperature, superimposed with addition damping peaks (Fig. 2). During the first heating two distinctive damping peaks at about 700 and 900 °C can be resolved, while during cooling only the peak at the lower temperature appears. It is noteworthy, that the peak at lower temperatures is much more pronounced during cooling than during the first heating. A second run of the IET cycle (Fig. 2b, specimen B2) only exhibits the peak at lower temperatures, similarly strong during heating and cooling, and no peak at higher temperatures.

Figure 4 shows the peaks during heating after subtracting the exponential background. This background was calculated by $D = A \exp(-U/kT)$ [10], with an apparent activation energy U. This apparent activation energy turned out to be between 1.0 and 1.2 eV. During the first heating cycle all as-fabricated specimens exhibit a double peak between 500 and 1000 °C, as exemplarily shown for specimen B1. During the second heating cycle only a very strong peak centered on 700 °C appears (B2). In the case of martensite structure (F1) the second peak centered around 900 °C is very dominant.

Microstructure

As fabricated, the microstructure of the SMD specimens consists mainly of a Widmanstätten structure with fine α phase lamellae (gray contrast) in a β phase matrix (white contrast) (Fig. 5a). Details about the microstructure of SMD specimens can be found elsewhere [5]. The microstructure after heat treatment at 1100 °C followed by quenching exhibits only a very low contrast, but nevertheless a very fine needle structure can be discerned (Fig. 5b). This low contrast can be explained by the fact that due to quenching from the β phase field, a martensitic structure is formed. Since the martensitic transformation is diffusionless, no material contrast appears, but only orientation contrast.

After IET up to 1100 °C, three different regions can be observed (Fig. 5c and d): an α/β Widmanstätten microstructure inside the specimens (Fig. 5d), a surface layer approximately 50 µm thick consisting of large, equiaxed, single phased α grains, and a very thin oxide layer on top of this. Such single phase α surface layer is well known for Ti alloys and called α casing [11–14]. It develops for example during machining in oxygen containing atmosphere. The α casing is most unwelcome, since it is very brittle. This agrees with the observation of many cracks within the α casing (Fig. 5c). The lamellae of the Widmanstätten microstructure inside the IET tested specimens are coarser than the ones in the as-fabricated state (compare Fig. 5a and d).

The amount of Ti, Al, and V of the different phases has been measured with EDX for specimens subjected to different thermal history. Figure 6 shows the results of point analyses of the α and β phase before and after IET. The α phase lamellae in the as-fabricated state have a higher V and a lower Al content than the one after exposure to high temperatures. The β phase generally exhibits a much larger

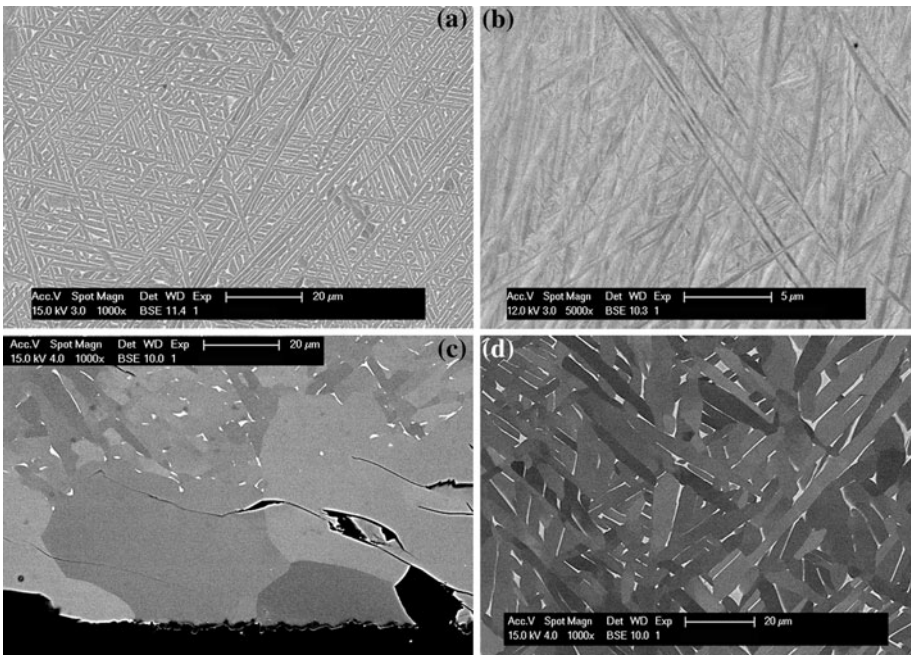

Fig. 5 Backscattered secondary electron micrographs of the as-fabricated SMD material (**a**), after heat treatment at 1100 °C and quenching (**b**), after IET testing up to 1100 °C of specimen E1 in overview at the surface (**c**) and inside the specimen (**d**)

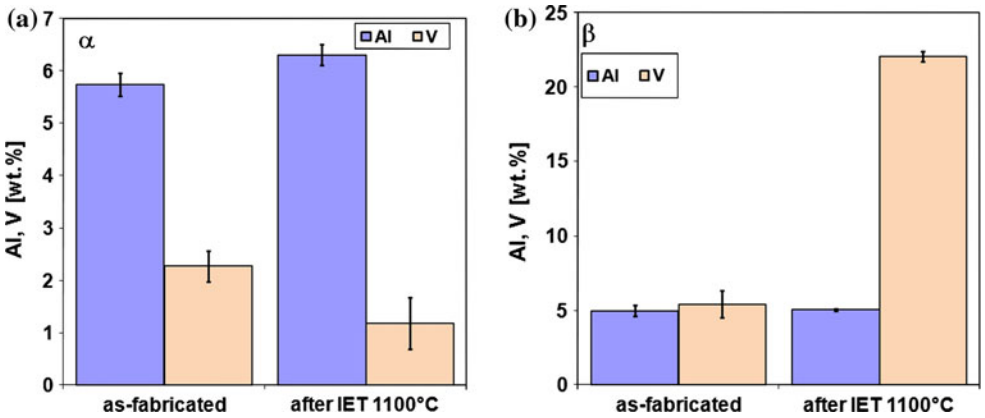

Fig. 6 Amount of V and Al of the α (**a**) and β phase (**b**) in the as-fabricated state and after IET; measured by EDX in the center of the specimens

amount of V and a somewhat lower amount of Al than the α phase. However, these values must not necessarily give the exact composition, since due to the small extent of the β phase compared to the cross section of the electron beam, especially in the as-fabricated state, the results may be falsified by the influence of the α phase in the vicinity. Nevertheless, while the exact values cannot be determined by this method, it is clear that the exposure to high temperatures increases drastically the concentration of V and decreases the concentration of Al in the β phase.

In contrast to EDX the EPMA-WDS microprobe can also determine oxygen. Measurements show an O concentration of 7 wt% near the surface, while in the center of the IET specimen no O is traceable.

The IGA, however, is more sensitive in measuring in light elements. Measurements with this technique show that in the as-fabricated state the SMD component has a similar amount in N and O as the wire (Table 1). After IET, however, the amount in O has more than doubled to a value of 0.370 wt%.

Microhardness

Similar to the microstructure, the micro-hardness in tested specimens changes dramatically due to the IET experiment. The Vickers hardness of the SMD specimens changes from 311 ± 25 HV0.1 in the as-fabricated state to 512 ± 41 HV0.1 after IET (center of the specimens). The heat treatment at 1100 °C followed by quenching has increased the hardness to 393 ± 12 HV0.1.

Furthermore, the IET tested specimens exhibit a hardness gradient between surface and center. Near the surface

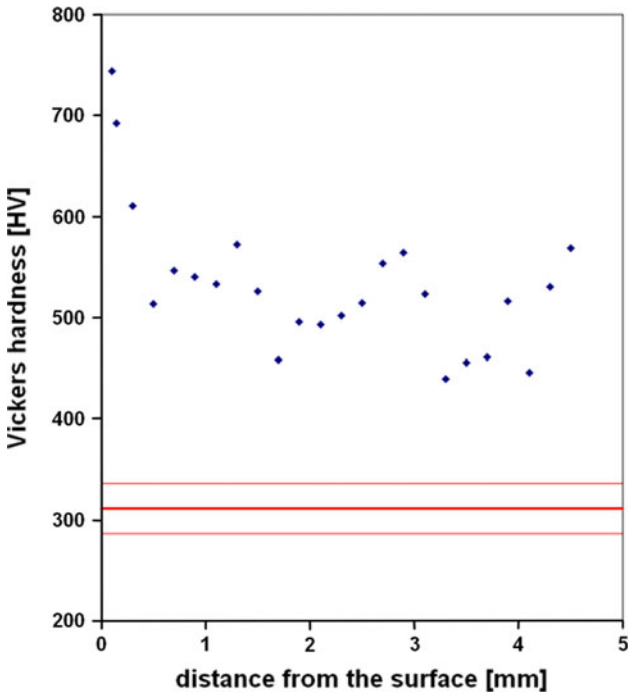

Fig. 7 Vickers micro-hardness in dependence on the distance from the surface (cross section of IET tested SMD specimen A). The horizontal lines indicate the average hardness of as-fabricated SMD material and the variance

within the α casing, the values of the measured specimens are very high (between 688 and 891 HV) decreasing continuously toward the center and reaching a constant value (Fig. 7). It is remarkable, that these values in the center are still much higher than the values measured before IET testing. Apparently, the material has hardened throughout the cross section due to the testing. A similar increase in hardness after heat treatment in air is described for commercially available Ti–6Al–4V, which was attributed to the dissolution of diffusing oxygen [15, 16].

Discussion

Young's modulus and damping

The dependence of Young's modulus and damping on temperature can be used to determine transformation and reaction processes, since both are sensitive indicators of phase changes and structural changes within the phases [9]. Damping is the more complex mechanical property, because it may depend on several mechanisms of energy dissipation. Damping peaks are often correlatable to modulus changes as a function of temperature or phase changes [9].

Welding processes can introduce residual stresses during the transition from liquid to solid state and in addition due to solid state phase transitions during further cooling. An important factor for the development of residual stresses is the constraint of the welded material with the much colder base material. In the case of SMD the constraining part is the cold base plate and in addition already deposited material. The free surfaces of a SMD component limit, however, the constraint and therefore residual stresses. Furthermore, during the SMD process the material is subjected repeatedly to high temperatures which possibly lead to stress relieve. In addition, while during the machining of the IET specimens the introduction of residual stresses was avoided by applying electrical discharge machining and manual grinding and polishing, the cutting of new surfaces is expected to lead to additional stress relieve. Hence, not much residual stress is expected in SMD IET specimens. This agrees with the results from X-ray diffraction measurements, where the residual stresses were found to be smaller than 200 MPa. Hence, an increase of damping due to residual stresses is assumed to be negligible for the present specimens.

The temperature dependence of the Young's modulus during heating is rather peculiar and shows three different stages, namely a gradual decrease until 900 °C, a strong decrease until 980 °C, and a plateau until the highest temperature was reached. During cooling essentially first a strong increase followed by a gradual increase is observed. Similar behavior during heating was already reported for pure Ti [17] and for Ti–6Al–4V [18]. The pure Ti was tested in a vacuum stated to be better than 1.3×10^{-4} mbar [17], while the other experiment was performed in an Ar atmosphere with unspecified purity at ambient pressure [18]. Unfortunately both articles do not show results for cooling and also do not present the microstructure of tested specimens making it impossible to decide about possible microstructural changes.

The damping shows an exponential increase with temperature and two peaks, the first peak between 600 and 900 °C during heating and cooling, and in addition a second peak around 960 °C during the first heating. In literature several damping peaks at different temperatures were described for Ti–6Al–4V. They have been attributed to dislocation breakaway from point defects (peak at −160 °C) and to the rearrangement of interstitial oxygen atoms (peak at 325 °C) [9]. At high temperature three further damping peaks were reported between 750 and 1030 °C, but were not explained [18].

In the following, explanations for the observed behavior of the Young's module and of the damping in dependence with the temperature will be presented.

α/β Transformation

One very important process for Ti–6Al–4V is the α to β transformation during heating, respectively, the β to α

transformation during cooling. The equilibrium $\alpha + \beta$ phase field of uncontaminated Ti–6Al–4V is reported to be between 600 and 980 °C [19, 20] with an Al rich and V lean α phase and an Al lean and V rich β phase. Possibly, the well-known phase diagram [19] does not apply for higher cooling rates as observed for SMD, and a smaller $\alpha + \beta$ phase field during rapid cooling must be considered [21]. In such a case, the α phase would be richer in V and leaner in Al than predicted for the equilibrium case. This argumentation is supported with the observation of different compositions of the α phase in the as-fabricated state (high cooling rates of the SMD process) and after IET (slow cooling rate of 2 °C/min, which can be considered as near equilibrium state).

Very fast cooling may in addition result in a martensitic transformation into the α' phase [22]. Performing SMD, the component is subjected repeatedly to a complex temperature field where, just after deposition, locally cooling rates high enough for the martensitic transformation can occur. However, no indications for martensites in SMD material can be found by microstructural analysis [5]. The reason for that could be the instability of the martensitic α' phase at high temperatures. It is reported that at temperatures below the β transus but above the martensite transition temperature, the martensite transforms diffusionally into the α and β phase [23, 24]. Modeling the temperature history of the SMD process shows that while at very high temperatures certainly the cooling rate is sufficiently high for the formation of α', during further cooling the transformation from the martensite into a $\alpha + \beta$ Widmanstätten structure takes place [25]. At room temperature less than 1% of α' phase at room temperature are predicted [25]. It is therefore imaginable that during the SMD process, $\alpha + \beta$ Widmanstätten structures may develop either directly $\beta \rightarrow \alpha + \beta$, or indirectly via an intermediate step of martensite transformation $\beta \rightarrow \alpha' \rightarrow \alpha + \beta$, depending on the local thermal history. These two Widmanstätten structures then would have different compositions, since the transformation has taken place at different temperatures allowing for the direct formation more diffusional separation than for the indirect formation. Unfortunately an exhaustive composition analysis to prove this hypothesis does not yet exist.

During IET, these phases with different compositions may naturally also exhibit different temperatures to transform into β. It has been shown by time-resolved X-ray diffraction that the transformation during heating closely follows the equilibrium phase diagram even at a relatively high heating rate of 20 °C/s [26]. The heating rate of the IET experiments is much slower and therefore this phase diagram can be applied. Starting with different compositions the transformation into the β phase takes place in different temperature regimes leading to two damping peaks as observed for the as-fabricated SMD specimens. During the slow IET cooling and during a subsequent heating and cooling sequence, equilibrium is obtained and only one damping peak occurs. The specimen heat treated at 1100 °C and water quenched before IET, naturally has experienced much less compositional separation and consists mainly of martensitic α' phase. Accordingly, mainly one damping peak appears around 900 °C (Fig. 4), which may tentatively be associated with the non-equilibrium α to β transformation peak.

The damping peaks reported in literature [18] between 750 and 1030 °C probably have to be attributed to α/β transformation, but it is not clear whether three peaks are visible due to a better resolution exhibiting transformations of α phases with different compositions, or whether they must be related to experimental imperfections.

It is noteworthy, that the α/β transformation apparently does not influence the trend of the Young's modulus between room temperature and 900 °C. The transformation starts at 600 °C and at 900 °C, it is expected that the β phase is the dominant phase. Hence, the severe change between 900 and 980 °C cannot be attributed to the α/β transformation. Therefore, it may be concluded that α- and β-phase apparently do not show a significant difference in the Young's modulus.

O alloying

Another process one has to consider is O alloying at high temperatures, which leads to α casing [11, 12, 14]. Ti alloys are very sensitive to O contamination and apparently the vacuum in the IET experiments was not good enough to prevent this. Oxygen acts as an α stabilizer for Ti–6Al–4V, decreases the volume fraction of β phase at all temperatures and raises the β transus temperature [27, 28]. Furthermore, oxygen increases the strength, the elastic modulus, and the hardness by interstitial solution strengthening [27, 28]. It must be pointed out, that the region of O alloying may be much deeper than the α case, and that the dimension of the α case only signifies the region where the O composition is high enough to prevent the β phase.

The raising of the β transus temperature by O is described by T_{tr} (°C) = 937 + 242.7* Oxygen (wt%) [27]. The α transus temperature seems to be less sensitive to the O concentration [29]. The O concentration was determined to be 0.15 wt% for the as-fabricated SMD component and 0.37 wt% after IET experiment. This would shift the β transus temperature from 973 to 1027 °C. Most O alloying is expected to occur at high temperatures in the β phase field. Therefore, the onset of the β to α transformation during cooling should be at higher temperatures than the end of the α to β transformation during the earlier heating

with less O. However, since during heating the two damping peaks are overlapping, this shift is not possible to be discerned.

As mentioned O alloying increases the hardness, which is reflected in the hardness gradient observed in IET tested specimens (Fig. 7). Correlating the increase in hardness with the determined O concentration before and after the IET experiment gives a good agreement with literature values (Fig. 8).

O alloying may have an influence on the Young's modulus measured by IET, which is a surface sensitive technique. Interstitial and substitutional α-stabilizing solutes such as O increase the Young's modulus, whereas β-stabilizing solutes decrease the modulus [30]. The diffusion of O is easier in body-centered cubic β phase than in close-packed hexagonal α or α' phase [31] facilitating the O alloying at temperatures above the β transus. This stiffening may be the reason for the plateau observed for the Young's modulus during heating at temperatures above the β transus temperature of about 980 °C. When cooling down, the Young's modulus increases and no plateau shows up. This indicates a permanent change in material properties. Accordingly, after the IET testing the Young's modulus has a higher value than before. Even after removing the α case by grinding for a second test, the Young's modulus is higher than in the as-fabricated state. Hence, the material was changed throughout the specimen, which agrees with the elevated O concentration after IET. During a second testing no plateau appears and almost no hysteresis develops, possibly indicating a saturation of the O concentration.

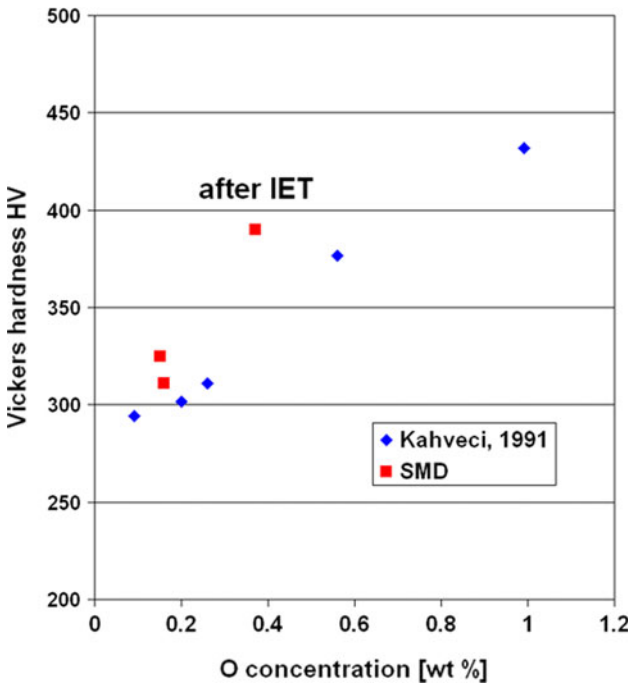

Fig. 8 Correlation between Vickers micro-hardness and O concentration of SMD specimens compared with literature [28]

Other authors have attributed the plateau observed for pure Ti to structural stabilization with temperature increase [17]. According to these authors, the bcc phase is unstable just above the transformation temperature and further temperature increase decreases the instability leading to increased stiffness and setting off the usual temperature-induced softening. However, it is questionable, whether this process would work effectively from 980 to 1150 °C. Unfortunately, these authors do not report about microstructure and possible α casing. Yet, the pressure inside their experimental set-up was kept in the order of 1.3×10^{-4} mbar, which is comparable with the vacuum of the present set-up. Therefore, also α casing is expected in their case.

Grain boundary softening

The strong decrease of the Young's modulus at elevated temperatures could be attributed to grain boundary softening [17]. Other authors speculate about a distinct change due to a "strain point" at which superplasticity begins to occur, but do not specify this process in detail [18].

The hypothesis of grain boundary softening is supported by the strong increase of the damping in this region, which is a common feature of many materials and can be ascribed to viscoelastic relaxation [32]. The magnitude of the high-temperature background is highly structure sensitive [33]. Exponential background can be caused by grain boundary softening and consequently results in viscous slipping of neighboring grains with respect to each other. From the exponential increase of the damping, an apparent activation energy between 1.0 and 1.2 eV can be derived.

Conclusion

The temperature-dependent Young's modulus and damping behavior of Ti–6Al–4V prepared by SMD is complex. The Young's modulus decreases gradually during heating until 900 °C, respectively, increases gradually during cooling from 900 °C, not reflecting the α/β transformation occurring at this temperature. The steep decrease of the Young's modulus between 900 and 980 °C is attributed to grain boundary softening. The plateau at higher temperatures is related to the stiffening by oxygen alloying. The damping peak around 700 °C during heating and cooling is ascribed to α/β transformation of a composition in thermal equilibrium. The damping peak around 900 °C, occurring only during the first heating sequence, is attributed to the transformation of a V rich and Al poor non-equilibrium α phase related with the fast cooling of the SMD process.

Acknowledgements The research is performed within the RAPOLAC STREP project under contract number 030953 of the 6th Framework Programme of the European Commission (www.RAPOLAC.eu), which is gratefully acknowledged. The support of Prof. Keith Ridgway and Dr. Rosemary Gault and her team at AMRC, Sheffield, United Kingdom, where the components have been built is highly appreciated.

References

1. Collings EW (1984) The physical metallurgy of titanium alloys. ASM International, Materials Park, Ohio
2. Long M, Rack HJ (1998) Biomaterials 19:1621
3. Clark D, Bache M, Whittaker M (2008) J Mater Process Technol 203:439
4. Baufeld B, van der Biest O (2009) Sci Tech Adv Mat 10:10. doi: 10.1088/1468-6996/10/1/015008
5. Baufeld B, Van der Biest O, Gault R (2009) Int J Mater Res 100:1536
6. Roebben G, Basu B, Vleugels J, van Humbeeck J, van der Biest O (2000) J Alloys Comp 310:284
7. Roebben G, Bollen B, Brebels A, van Humbeeck J, van der Biest O (1997) Rev Sci Instrum 68:4511
8. ASTM (1999) E 1876:1075
9. Lee YT, Welsch G (1990) Mat Sci Eng A 128:77
10. Riviere A (2001) Mat Sci Forum 366–368:268
11. Rosen A, Rottem A (1976) Mater Sci Eng 22:23
12. Satyanarayana DVV, Pandey MC (1991) Scr Met Mat 25:2273
13. Evans RW, Hull RJ, Wilshire B (1996) J Mater Process Technol 56:492
14. Patankar SN, Kwang YT, Jen TM (2001) J Mater Process Technol 112:24
15. Borgioli F, Galvanetto E, Galliano FP, Bacci T (2001) Surf Coat Technol 141:103
16. Guleryuz H, Cimenoglu H (2005) Surf Coat Technol 192:164
17. Ogi H, Kai S, Ledbetter H, Tarumi R, Hirao M, Takashima K (2004) Acta Mater 52:2075
18. Fukuhara M, Sanpei A (1993) J Mater Sci Lett 12:1122
19. Boyer R, Welsch G, Collings EW (1994) Materials properties handbook: titanium alloys. ASM International, Materials Park, Ohio
20. Qian L, Mei J, Liang J, Wu X (2005) Mater Sci Technol 21:597
21. Banerjee R, Collins PC, Bhattacharyya D, Banerjee S, Fraser HL (2003) Acta Mater 51:3277
22. Ahmed T, Rack HJ (1998) Mater Sci Eng A 243:206
23. Gil FJ, Ginebra MP, Manero JM, Planell JA (2001) J Alloys Comp 329:142
24. Qazi JI, Senkov ON, Rahim J, Froes FH (2003) Mater Sci Eng A 359:137
25. Fachinotti VD, Cardona A, Baufeld B, Van der Biest O (2010) In: Dvorkin E, Goldschmit M, Storti M (eds) Mecanica Computacional, vol XXIX. Asociacion Argentina de Mecanica Computacional, Buenos Aires
26. Babu SS, Kelly SM, Specht ED, Palmer TA, Elmer JW (2005) In: Howe JM, Laughlin DE, Lee JK, Lee JK, Dahmen U, Soffa WA (eds) International conference on solid-solid phase transformations in inorganic materials (PTM 2005). Minerals, Metals & Materials Society, Phoenix
27. Kahveci AI, Welsch GE (1986) Scr Met Mat 20:1287
28. Kahveci AI, Welsch GE (1991) Scr Met Mat 25:1957
29. Malinov S, Sha W, Guo Z (2000) Mat Sci Eng A 283:1
30. Conrad H (1981) Prog Mater Sci 26:123
31. Wang W, Wang M, Jie Z, Sun F, Huang D (2008) Opt Lasers Eng 46:810
32. Weller M, Chatterjee A, Haneczok G, Clemens H (2000) J Alloys Comp 310:134
33. Nowick AS, Berry BS (1972) Anelastic relaxation in crystalline solids. Academic Press, New York